Published in final edited form as:

Neuroscience. 2015 June 4; 295: 1–10. doi:10.1016/j.neuroscience.2015.03.018.

Forebrain neuronal specific ablation of p53 gene provide protection in a cortical ischemic stroke model

Emily Filichia, BA[1], **Hui Shen, MD**[2], **Xiaofei Zhou, BA**[1], **Xin Qi, PhD**[3], **Kevin Jin**[1], **Nigel Greig, PhD**[4], **Barry Hoffer, MD PhD**[1], and **Yu Luo, PhD**[1]

[1]Department of Neurological Surgery, Case Western Reserve University, Cleveland, USA

[2]National Institute of Drug Abuse, Baltimore, USA

[3]Department of Physiology, Case Western Reserve University, Cleveland, USA

[4]National Institute of Aging, Baltimore, USA

Abstract

Cerebral ischemic injury involves death of multiple cell types at the ischemic sites. As a key regulator of cell death, the p53 gene has been implicated in the regulation of cell loss in stroke. Less focal damage is found in stroke animals pre-treated with a p53 inhibitor or in traditional p53 knockout (ko) mice. However, whether the p53 gene plays a direct role in regulating neuronal cell death is unknown. In this study, in contrast to the global inhibition of p53 function by pharmacological inhibitors and in traditional p53 ko mice, we utilized a neuronal specific conditional ko mouse line (CamcreTRP53 $^{loxP/loxP}$) to achieve forebrain neuronal specific deletion of p53 and examined the role of the p53 gene in ischemia-induced cell death in neurons. Expression of p53 after stroke is examined using immunohistochemical method and outcome of stroke is examined by analysis of infarction size and behavioral deficits caused by stroke. Our data showed that p53 expression is upregulated in the ischemic region in neuronal cells in wildtype (wt) mice but not in CamcreTRP53 $^{loxP/loxP}$ ko mice. Deletion of the p53 gene in forebrain neurons results in a decreased infarction area in ko mice. Locomotor behavior, measured in automated activity chambers, showed that CamcreTRP53 $^{loxP/loxP}$ ko mice have less locomotor deficits compared to wt mice after MCAo. We conclude that manipulation of p53 expression in neurons may lead to unique therapeutic development in stroke.

Keywords

conditional p53 knockout; stroke; neuroprotection

Correspondence to Yu Luo, PhD, Department of Neurological Surgery, Case Western Reserve University, 2109 Adelbert Rd, Cleveland, OH, USA. **yxl710@case.edu**, Phone: 01-216-368-4169.

Disclosures: None.

Introduction

Cerebral ischemic injury is multifactorial and involves cell death of multiple cellular components including neurons and glial cells (Choi, 1996, Love, 2003, Zheng et al., 2003). The tumor suppressor p53 plays an essential role in the regulation of cell death. It has been suggested that p53 might be involved in cell death that occurs in stroke (Hughes et al., 1997, Li et al., 1997, Culmsee and Mattson, 2005). p53 protein is reported upregulated after ischemic injury and leads to p53-dependent apoptosis at the ischemic sites (Li et al., 1994, Leker et al., 2004). Less focal damage is found in stroke animals pre-treated with a p53 inhibitor (Culmsee et al., 2001, Zhu et al., 2002, Leker et al., 2004) or in traditional p53 knockout (ko) mice (Crumrine et al., 1994). These data suggest that p53 is an important mediator of programmed cell death in the ischemic region. However, due to widespread inhibition of p53 genes by pharmacological inhibitors and the loss of p53 function in all cell types in traditional p53 ko mice, the pharmacological inhibitor and genetic linkage studies do not address the question as to whether p53 function determines the outcome of stroke by either directly regulating the cell death of neurons or through indirect modulation of the microenvironment in ischemic injury. To investigate whether p53 can directly regulate neuronal cell survival in ischemic injury, we generated transgenic mice carrying forebrain neuronal-specific ablation of the p53 gene and examined the role of p53 in neuronal death and functional outcome after neuronal specific p53 deletion in a cortical ischemic stroke model.

EXPERIMENTAL PROCEDURES

Animals

All animal protocols were conducted under National Institutes Health (NIH) Guidelines using the NIH handbook *Animals in Research* and were approved by the Institutional Animal Care and Use Committee of Case Western Reserve University. The mice were housed in the animal facility of Case Western Reserve University on a 12-h light/dark diurnal cycle. Food was provided ad libitum. Forebrain neuronal specific p53 deletion mice (Fig 1A) were generated by crossing $TRP53^{loxP}$ (Jonkers et al., 2001) mice with a mouse line that carries the cre gene under the control of the Camkinase II promoter (Minichiello et al., 1999) to generate CamcreTRP53 ko (cre+/$TRP53^{loxP/loxP}$) or wildtype (wt) mice (cre−/$TRP53^{loxP/loxP}$ or cre+/$TRP53^{wt/wt}$). The Camkinase cre gene was genotyped by primers (5' GGT TAG CAC CGC AGG TGT AG -3'; 5' CTA ATC GCC ATC TTC CAG CAG -3'). TRP53 floxed alles are genotyped by the primer set (5' CAC AAA AAC AGG TTA AAC CCA G-3'; 5' AGC ACA TAG GAG GCA GAG AC-3'). Deletion of the exon 1-10 of the p53 gene results in amplification of a ΔloxP band, which is amplified by a set of primers flanking the 5’ of exon 1 and 3’ of exon 10.

Cortical ischemia model (distal MCA occlusion)

Focal cerebral ischemia was produced in the mice using our procedure described previously (Shen et al., 2008, Luo et al., 2009). The mice were anesthetized with chloral hydrate (0.4 g/kg, i.p.). Body temperature was monitored and maintained at 37 °C degrees by a heating pad. The surgical area was shaved and prepared with alternating betadine scrubs and ethanol.

A small 5-mm vertical skin incision was cut between the right eye and ear to expose the skull. A small window was drilled open in the skull to expose the middle cerebral artery (MCA). The right MCA was ligated with 10-0 suture for 90 min followed by removal of the ligating suture to allow for reperfusion. The skin wound was closed with suture and the mice were placed in a heated animal intensive care unit chamber until recovery of the righting reflex.

Behavioral tests

Locomotion function was measured before stroke and 48 hr after stroke in CamcreTPR53 ko (n= 16) and wt (n=17) mice. Voluntary locomotor functions were examined using automated infrared locomotor activity chambers, as previously described (Luo et al., 2009). Locomotor function was assessed by a 30 min trial in an open field crossed by a grid of photobeams (VersaMax system, AccuScan Instruments). Counts were taken of the number of photobeams broken during the trial at 5 min intervals, with separate measures for total horizontal activity and total movement time. Total horizontal activity corresponds to the total number of beam interruptions that occurred in the horizontal sensor during a given sample period and total movement time corresponds to the amount of time that animal was in ambulation during a given sample period. Other locomotor parameters are listed in Table 1.

Experimental timeline

Male adult (3-4 months old) CamcreTRP53 ko and wt mice were initially subjected to baseline locomotion function. At 48 hr after stroke, animals were subjected to post-stroke locomotion examination. After the behavioral tests, ko and wt mice were perfused with 4% paraformaldehyde (PFA) and the brains were immunostained with both an anti-NeuN antibody and cresyl violet Nissl staining as described (Fujimoto et al., 2008) to assess the area of neuronal loss. The brain sections were also immunostained with anti-p53 and anti-MAP2 antibody to examine the expression of p53 protein in the contralateral and ipsilateral sides of the brain, as detailed below.

Immunohistochemistry and infarction area quantification

Mice were perfused transcardially with a solution of 4% PFA (pH 7.2) in 0.1 M phosphate buffer (PB, pH 7.2). Brains were removed from the skull, postfixed in 4% PFA overnight at 4 °C, rinsed with PB, and sequentially transferred to 30% sucrose in 0.1M phosphate buffer, pH 7.2 solutions over night. Brains were frozen on dry ice and sectioned on a cryostat to obtain coronal sections of 25 μm in thickness.

Sections were rinsed with PB prior to processing for immunocytochemistry, blocked in PB containing 4% bovine serum albumin (BSA), 0.3% Triton X-100 and 10% goat serum for 1 hr at RT followed by incubation with mouse anti-NeuN primary antibody (Millipore, 1:500) for 24 hr at 4°C. Primary antibody dilutions were in PB containing 1% BSA, 0.3% Triton X-100 and 1% goat serum. After rinsing 3×10 min in PB, sections were processed with an ABC kit (Vector Laboratories, Burlingame, CA). Sections were then incubated in a 1:200 dilution of the biotinylated anti–mouse secondary antibody. After rinsing with PB, sections were incubated with avidin-biotinylated horseradish peroxidase for 1 hr. Samples were rinsed and the peroxidase reaction was developed with 0.05% 3,3-diaminobenzidine-4 HCl

(DAB) and 0.003% hydrogen peroxide (H_2O_2). Sections were mounted on coated slides, air dried, dehydrated in 75%, 95% and 100% ethanol followed by 10 min Xylene. The slides were coverslipped for viewing under polarized light microscope. Images were captured with the microscope (Leica Microsystem Inc. Bannockburn, IL) and the infarcation area in each animal was quantified using NIS element software by blinded observers. The boundaries of neuronal degeneration were outlined by loss of NeuN staining in the cortex. The total area on the contralateral side was measured and subtracted by the total surviving area in the stroke side to calculate the infarction area. This method minimizes the potential error that might be introduced by edema by measuring the volumes of the surviving, noninfarcted tissue rather than the volumes of the infarcted tissue per se (Swanson et al., 1990). A set of adjacent sections were subjected to cresyl violet Nissl staining and the infarct area in each animal was quantified using the same method as described above. Immunoflurescent staining of p53 (monoclonal, Cell Signaling) and MAP2 (polyclonal rabbit, Millipore) protein was carried out with similar methods as described above with the exception of the antigen-retrieval process and the use of a fluorescent secondary antibody. Activated astrocytes and microglial cells were identified using anti-GFAP (monoclonal, Sigma) and Iba1 (rabbit, Wako) antibodies followed by incubation with fluorescent secondary antibodies. Omission of primary or secondary antibodies resulted in no staining and served as negative controls. Activated astrocytes and microglial cells were quantified by counting 5 randomly selected counting frames (40X) expanding the infarct boundary for each animal and the average of total positive cells per field was calculated for each animal. For activated microglial cell body size measurement, the cell body diameter was measured using NIS element software by blinded observers and an average of 30 cells were measured for each animal. A total of 5 wt and 5 ko mouse brains were analyzed to quantify activated astrocytes and microglial cells.

Stereological counts of neuronal density in cortical layers of wt and CamcreTPR53 ko mouse brains

Unbiased stereological counts of NeuN-positive neurons within each layer of the somatosensory and motor cortex were performed using unbiased sterological principles and analyzed with StereoInvestigator software (Microbrightfield, Williston, VT). Optical fractionator sampling was carried out on a Leica DM5000B microscope (Leica Microsystems, Bannockburn, IL) equipped with a motorized stage and Lucivid attachment (40X objective). The neuronal cell density in each layer was measured using unbiased stereological principles. Different layers of cortical layers I through VI of the neocortex in the somatosensory and motor cortex area were outlined according to neuronal cell type, shape and density. Basically, Layer I (molecular layer) is located underneath the meninges and consists of neuropil and few cell bodies of neurons. Layer II/III contains many granule (stellate) cells (small interneurons) and numerous cone-shaped cell bodies of small pyramidal cells. Layer IV (internal granular layer) is composed of granule cells. Layer V (internal pyramidal layer) contains cell bodies of large pyramidal cells. Layer VI (fusiform or multiform layer) is dominated by elongated spindle-shaped (fusiform) cells. For each tissue section analyzed, section thickness was assessed at each sampling site and a guard zone of 2.5μm was used at the top and bottom of each section. Pilot studies were used to determine suitable counting frame and sampling grid dimensions prior to counting. The

following stereolgic parameters were used in the final study: grid size, (X) 220 μm, (Y) 166 μm; Counting frame, (X) 68.2 μm, (Y) 75 μm, depth was 20 μm. Gundersen coefficients of error for m=1 were all less than 0.10. Stereologic estimations were performed with the same parameters in all layers of wt or CamcreTRP53 ko mice (n=4 for each genotype).

Statistics—Statistical analysis was performed using Student's *t* test, and one- or two-way analysis of variance (ANOVA) as appropriate, with Newman–Keuls post hoc tests. *p* values less than 0.05 were considered significant.

Results

In our transgenic model, Cre recombinase expression is driven by the Camkinase promoter and many studies have used this mouse line to evaluate forebrain neuronal specific gene deletion in mice. To determine the specific deletion of the mTRP53 gene in forebrain, primers specific to the recombination (ΔloxP) were used to amplify the recombined TRP53 allele. As expected, only tissue obtained from the cortex, striatum, olfactory bulb and hippocampus contained ΔloxP, confirming the deletion of the p53 gene in these brain areas. In contrast, the cerebellum, that was previously reported to have no or minimal recombination (Minichiello et al., 1999), was found to be negative for recombination PCR product, indicating lack of p53 gene deletion in cerebellum in our CamcreTRP53 mice. (Fig 1B upper panel). All brain tissues from different regions were also subjected to PCR reactions that detected the loxP flanked allele to confirm the quality of DNA as well as the genotype of ko mice (Fig 1B lower panel).

The CamcreTRP53 ko mice were born at expected Mendelian frequencies and showed normal viability. The body weights of adult ko and wt mice were not significantly different (wt= 26.6±0.8, ko= 27.2±0.5; p=0.58, n=16). Additionally in adult mice, no apparent differences in the general structure and density of cortical neurons were noted between wt and ko animals (Figs 2B, 2C and 2D show representative images of motor cortex in wt and ko mice). Unbiased stereological counts of NeuN positive cells in layer layers I through VI somatosensory and part of the motor cortex showed no difference in neuronal cell density in various layers between wt and CamcreTRP53 ko mice (Fig 2E and 2F). Basal locomotion tests performed prior to stroke at age 3-4 months in automated behavioral chambers did not reveal any difference between the ko and wt mice (total horizontal activity – the total number of beam interruptions that occurred in the horizontal sensor during 30 min, wt=13255.9±845.6, n=17; ko=14573.6±845.6, n=16; p=0.246; total movement time - the amount of time that animal was in ambulation during 30 min, wt=662.3±9.2, n=17; ko=732.3±43.8, n=16; p=0.271). Distal MCA occlusion resulted in p53 protein upregulation in the penumbra on the stroke side but not in the contralateral cortex (Fig 3). Interestingly, wt mice showed induction of p53 protein both within neurons (arrow in Fig 3 panel i right, 48% of p53 positive cells) and other cell types (arrow head in Fig 3 panel i right, 52% of p53 positive cells, total of 150 p53 positive cells counted). However, in CamcreTRP53 ko mice, p53 protein expression was only observed in the penumbra mainly in cells that were MAP2 negative (Fig 3 ii right, arrow head, 82% of total p53 positive cells are MAP2 negative) suggesting that the p53 gene is upregulated in other cell types in CamcreTRP53 ko mice but not in neurons in stroke brain. We also found some surviving MAP2 positive neurons near

the ischemic core that were p53 negative (Fig 3iii, small arrow) whereas other non neuronal cells that were in the same optical field were p53 positive (Fig 3iii, arrow head). These data confirm that p53 protein is induced in stroke brain both in neurons and non neuronal cells, but are not expressed in cortical neurons in CamcreTRP53 ko mice.

Distal MCA occlusion causes infarction in cortex that can be revealed by both Nissl staining and NeuN immunostaining. Quantification of the infarction area in cortex showed that neuronal deletion of the p53 gene results in a smaller infarction size in ko mice measured by both Nissl staining (59.7±11.9% compared to wt mice 100±10.6%; n=15; p=0.014, Fig 4A and 4B) and NeuN immunostaining (49.4±8.1% compared to wt mice 100±12.3%; n=15; p=0.0018, Fig 4C). More importantly, motor behavioral function analysis measured by automated open field chambers showed that p53 deletion in neurons in ko mice resulted in less severe motor function deficits in ko mice as demonstrated by total horizontal activity– the total number of beam interruptions that occurred in the horizontal sensor during 30 min, (see Fig 5B; wt=6469.8±619.1, n=17; ko=9301±780.6, n=16; p=0.013, two-way ANOVA), total movement time – the amount of time that animal was in ambulation during 30 min, (see Figure 5C; wt=322.94±28.1, n=17; ko=485.16±41, n=16; p=0.003). All the major 8 variables showed similar results in that CamcreTRP53 ko mice have less deficits in motor function after distal MCAo (see Table 1).

Since activated astrocytes and microglial cells are important elements in brain tissue damage after ischemia, we also investigated whether neuronal deletion of p53 gene alters the astrocytes and microglial cell components in stroke mice. We found that both reactive astrocytes (identified by GFAP immunoreactivity) and activated microglial cells (identified by Iba1 immunoreactivity and morphological changes such as increased cell body size and shortened cellular processes) are present at the infarct boundary, with microglial cells located closer to the ischemic area surrounded by GFAP positive cells in the outer layer (Fig 6A). We also quantified the density of GFAP positive and Iba1 positive cells in the activated infarct boundary and found that the density of GFAP positive cells (Fig 6B) and Iba1 positive cells (Fig 6C) at the infarct boundary showed no difference between the wt and ko mice. However, the average size of activated microglia (measured by diameter of Iba1 cells) was smaller in ko mice compared to wt mice (see Fig 6 D, wt=59.3±2.8 pixels; ko=51.4±1.7 pixels; p=0.04. n=5 for wt and ko mice, >30 cells measured for each mouse).

Discussion

p53 protein expression and function have been implicated in the cellular and molecular mechanisms of ischemic injury in many previous studies (Crumrine et al., 1994, Zhu et al., 2002, Culmsee and Mattson, 2005). Once activated, p53 increases transcription of a variety of key genes involved in the development of programmed cell death that comprise pro-apoptotic members of the Bcl-2 family (Bax, Bad, Bid, Noxa, Puma) involved in mitochondrial outer membrane permeablilization, apoptotic protease-activating factor 1 (APAF1) as well as other apoptosis regulatory proteins such as SIVA1 (Culmsee and Mattson, 2005, Chatoo et al., 2011, Smith et al., 2013). Additionally, p53 has transcription-independent proapoptotic actions, including association with mitochondria (Marchenko et al., 2000), resulting in outer membrane permeabilization and consequent release of

mitochondrial proapoptotic factors into the cytosol, such as cytochrome *c* and Smac/DIABLO; these activate caspase-dependent apoptosis (Saelens et al., 2004, Green, 2006, Nijboer et al., 2011). p53 expression is upregulated in ischemic brain (Li et al., 1994) as well as in other acute neurological insults, including traumatic brain injury (TBI) (Greig et al., 2004, Plesnila et al., 2007, Nijboer et al., 2011, Rachmany et al., 2013). The p53 inhibitor PFT-α delivered both before and post stroke attenuates ischemic injury and promotes the survival of regenerating cells after stroke (Crumrine et al., 1994, Luo et al., 2009) as well as TBI (Plesnila et al., 2007, Rachmany et al., 2013). Likewise, the use of PFT-μ, a small agent that inhibits the interaction of p53 with mitochondria without impacting its transcriptional activity, mitigates perinatal hypoxic-ischemic brain damage (Nijboer et al., 2011). Furthermore, general deletion of the p53 gene in traditional p53 ko mice or decreased dosage of p53 in heterozygous mice provides protection against ischemic injury (Crumrine et al., 1994). A recent study has reported that the human *Trp53 Arg72Pro* polymorphism helps explain different functional prognosis in stroke patients (Gomez-Sanchez et al., 2011). However, whether p53 function regulates neuronal cell death directly or through modulation of the microenvironment by controlling cell death of glia or other cells is unknown. In this study, using a forebrain neuronal specific p53 deletion mouse model, we evaluated the direct involvement of the p53 gene in neuronal cell death that occurs in ischemic injury. This strategy represents a significant advantage because it permits a specific evaluation of p53 function in these cells, compared to the non-selective effects of pharmacological inhibitors on multiple cell types in multiple anatomical regions, and at concentrations where agents such as PFT-α can potentially provide other actions (Neitemeier, 2014).

The role of p53 in the pathophysiology of central nervous system (CNS) injuries remains complex and warrants further elucidation, as a non-apoptotic role of p53 has been implicated in the promotion of neuronal and axonal regeneration after cellular insults (Tedeschi and Di Giovanni, 2009). Such a variety of actions can be attributed to factors such as the cell types, their microenvironment and both the form and severity of injury involved, in addition to when p53 activity and involved signaling pathways are evaluated. Models that permit the separation of these factors to allow the characterization of p53 action in neurons are thus valuable. The effectiveness of specific p53 deletion in forebrain but in no other brain regions was confirmed by PCR in CamcreTRP53 $^{loxP/loxP}$ ko mice (Fig 1). Loss of the p53 gene in forebrain neurons did not lead to an abnormal development of cortex, as demonstrated by the regular structure of the forebrain and normal neuronal cell density (NeuN positive cells) in ko mice (Fig 2). The Camkinase cre line has been utilized in many studies previously to specifically study the role of certain genes in forebrain neurons (Minichiello et al., 1999, Rios et al., 2001). It was reported that floxed gene recombination occurs at about postnatal day 20 (Dragatsis and Zeitlin, 2000). Because of no or minimal gene deletion during embryogenesis, this animal model enables us to examine the role of the p53 gene in adult neuronal cell death during stroke without potential confounding factors, such as possible developmental changes that occur within the general structure of the neocortex. Our data also suggest that the p53 gene might not be critical for the postnatal apoptotic processes that eliminate excess neurons during postnatal development (Kim and Sun, 2011). Following the induction of a stroke, immunostaining showed that p53 protein is induced in both neurons and non-neuronal cells within the penumbra but not in the contralateral cortex (Fig 3).

However, in CamcreTRP53 ko mice, p53 expression was mainly detected in non neuronal cells at the penumbra (Fig 3). Interestingly, we also identified some surviving MAP2 positive neurons near the ischemic core that are p53 negative, suggesting that lack of p53 in these neurons might contribute to their survival within the penumbra. Indeed, we found that loss of p53 in forebrain neurons in adult mice proved protective against ischemic injury after stroke (MCAo). CamcreTRP53 ko mice showed smaller infarction areas compared to their wt littermates. Both Nissl staining and NeuN immunostaining were carried out to measure infarct size in this study. Nissl staining is a widely accepted and commonly used conventional histological technique to identify infarcts in stroke animals (Popp et al., 2009). NeuN immunostaining have recently been utilized to visualize neuronal cell loss in CNS injuries including stroke, especially selective neuronal loss (Liu et al., 2009, Baron et al., 2014, Emmrich et al., 2015). Both techniques demonstrated decreased infarct size in CamcreTPR53 ko mice compared to their wt littermates. Interestingly, NeuN immunostaining demonstrated a slightly smaller infarct size (49.4±8.1% compared to wt mice identified by NeuN immunostaining vs 59.7±11.9% compared to wt mice using Nissl staining). It has been shown that at earlier time points (6- 24 hours after MCAo), conventional histological techniques, such as Nissl or TTC, show similar results; however, NeuN immunostaining can recover at later time points (48 or 72 hours after MCAo) which might reflect transiently damaged neurons that later “regain their staining pattern after repair” (Liu et al., 2009). In our study, both stainings were carried out at 48 hours and neuronal deletion of p53 might result in recovery of initially damaged neuronal cells that lack p53 protein. This suggests that NeuN staining might be a more sensitive marker for measuring true neuronal damage. The surviving neurons close to core of the infarct area (peri infarct area) might play an important role in infarct growth and neurovasculature repair. Since damage to neurons and vasculature are the current predominant hypotheses in the “neurovascular” pathology of stroke, we speculate that the p53- deficient neurons in the peri infarct area might survive the initial ischemic insult and recover in later stages of infarct development. The surviving p53-deficient neurons might contribute to less depolarization, excitotoxicity and consequent inflammatory and neurovasculature damage which all play a critical role in pathological development in stroke (Shinozuka et al., 2013). Indeed, our data showed that although the cell density for activated astrocytes and microglia were not different between wt and ko mice, the size of microglia cell body, an indication of the extent of their activation (Eggen et al., 2013) is smaller in ko mice brain at the infarct boundary, suggesting that selective survival of p53-lacking neurons might lead to less inflammatory responses which could contribute to smaller infarct area and subsequent better recovery after stroke. It is possible that selective survival of neurons the in peri infarct area might also facilitate reestablishment of neuronal connections and repair of the neurovasculature in injured animals through regulation of various genes such as BDNF (Luo et al., 2013), ATRX, IGF1 and Lingo1: (Li et al., 2010). Although our study only analyzed infarction and neuronal survival at 48 hours after stroke, it will be valuable to follow these mice longer after ischemic onset to evaluate the effect of neuronal p53 gene deletion on the later development of stroke pathology.

Locomotor behavior, measured in automated activity chambers, showed that CamcreTRP53 ko mice have less locomotor deficits compared to wt mice after MCAo. Distal MCAo in

mice affects mostly the primary somatosensory cortex and part of the lateral motor cortex. Damage in these areas caused by distal MCAo results in compromised sensorimotor performance in rodents (Freret et al., 2009, Balkaya et al., 2013). The open field test is widely used to evaluate motor function and normal exploratory locomotion in rodents (Belzung and Griebel, 2001, Luo et al., 2009). In this study, we utilized an automated open field apparatus that minimizes disturbing effects induced by a human observer. Utilizing the same apparatus, our group has shown a positive correlation of infarct size at 48 hours post dMCAo and multiple parameters measured by this apparatus (Shen and Wang, 2010) in rats. In this study, all of the 8 main parameters measured demonstrated less severe deficits in CamcreTRP53 ko mice, except for total vertical activity (total number of beam interruptions in the vertical sensor) that showed a similar trend but was not statistically significant. Our initial investigation of reactive astrocytes and activated microglial cells suggests that improved neuronal survival in the peri infarct area in ko mice is correlated with reduced microglial activation. Microglial activation is associated with production of detrimental inflammatory factors (Perry et al., 2010) and is closely related to selective neuronal loss after ischemia (Baron et al., 2014, Emmrich et al., 2015). Recently, it has also been shown that microglial cells actually play dual and opposite roles in inflammatory response progression in stroke depending on whether they manifest an M1 (pro-inflammation and “injurious” phenotype) or an M2 (anti-inflammation and protective phenotype) (Hu et al., 2012). Therefore, additional analysis of the profile of classes of microglial cell activation and other potential pathological mechanisms, such as endothelium and neurovasculature repair, are warranted in future studies. In summary, our data suggest that loss of p53 function specifically in forebrain neurons can protect these cells from ischemic injury occurring after stroke, and add support to the notion that short-term transient inactivation of p53 might provide a new treatment strategy for improved prognosis in acute life-altering neurological disorders (Greig et al., 2004, Gudkov and Komarova, 2005). The use of tetrahydrobenzothiazole analogue p53 inhibitors (Zhu et al., 2002) and other newly synthesized analogues (Strom et al., 2006) has aid characterize the fundamental role of p53 in the biochemical cascades that lead to neuronal apoptosis across both cellular and animal models (Culmsee and Mattson, 2005, Gudkov and Komarova, 2010). These same agents have additionally demonstrated that this p53 mediated system is amenable to reversal by blocking the apoptotic cascade to mitigate neuronal loss in stroke, traumatic brain injury and epilepsy animal models (Zhu et al., 2002, Leker et al., 2004, Plesnila et al., 2007, Engel et al., 2010, Nijboer et al., 2011, Sano et al., 2012, Rachmany et al., 2013) when administered up to approximately 6 hours after the event. Our present study suggests that neuronal-specific, rather than a global p53 inhibition approach may achieve neuronal preservation with less potential adverse effects that may ensue (Gudkov and Komarova, 2010). Application of pharmacological inhibition of p53 in neuronal, glial or endothelial specific p53 gene deletion animal models may also provide valuable insights on the precise role of different cellular components in pathological development in stroke and should be considered for future studies.

Acknowledgments

Sources of Funding: Dr. Yu Luo is funded by the American Heart Association National Scientist Development Award. This work is supported in part by the Intramural Research Program of the National Institute on Aging, NIH.

References

Balkaya M, Krober JM, Rex A, Endres M. Assessing post-stroke behavior in mouse models of focal ischemia. Journal of cerebral blood flow and metabolism : official journal of the International Society of Cerebral Blood Flow and Metabolism. 2013; 33:330–338.

Baron JC, Yamauchi H, Fujioka M, Endres M. Selective neuronal loss in ischemic stroke and cerebrovascular disease. Journal of cerebral blood flow and metabolism : official journal of the International Society of Cerebral Blood Flow and Metabolism. 2014; 34:2–18.

Belzung C, Griebel G. Measuring normal and pathological anxiety-like behaviour in mice: a review. Behavioural brain research. 2001; 125:141–149. [PubMed: 11682105]

Chatoo W, Abdouh M, Bernier G. p53 pro-oxidant activity in the central nervous system: implication in aging and neurodegenerative diseases. Antioxidants & redox signaling. 2011; 15:1729–1737. [PubMed: 20849375]

Choi DW. Ischemia-induced neuronal apoptosis. Current opinion in neurobiology. 1996; 6:667–672. [PubMed: 8937832]

Crumrine RC, Thomas AL, Morgan PF. Attenuation of p53 expression protects against focal ischemic damage in transgenic mice. Journal of cerebral blood flow and metabolism : official journal of the International Society of Cerebral Blood Flow and Metabolism. 1994; 14:887–891.

Culmsee C, Mattson MP. p53 in neuronal apoptosis. Biochemical and biophysical research communications. 2005; 331:761–777. [PubMed: 15865932]

Culmsee C, Zhu X, Yu QS, Chan SL, Camandola S, Guo Z, Greig NH, Mattson MP. A synthetic inhibitor of p53 protects neurons against death induced by ischemic and excitotoxic insults, and amyloid beta-peptide. Journal of neurochemistry. 2001; 77:220–228. [PubMed: 11279278]

Dragatsis I, Zeitlin S. CaMKIIalpha-Cre transgene expression and recombination patterns in the mouse brain. Genesis. 2000; 26:133–135. [PubMed: 10686608]

Eggen BJ, Raj D, Hanisch UK, Boddeke HW. Microglial phenotype and adaptation. Journal of neuroimmune pharmacology : the official journal of the Society on NeuroImmune Pharmacology. 2013; 8:807–823. [PubMed: 23881706]

Emmrich JV, Ejaz S, Neher JJ, Williamson DJ, Baron JC. Regional distribution of selective neuronal loss and microglial activation across the MCA territory after transient focal ischemia: quantitative versus semiquantitative systematic immunohistochemical assessment. Journal of cerebral blood flow and metabolism : official journal of the International Society of Cerebral Blood Flow and Metabolism. 2015; 35:20–27.

Engel T, Murphy BM, Hatazaki S, Jimenez-Mateos EM, Concannon CG, Woods I, Prehn JH, Henshall DC. Reduced hippocampal damage and epileptic seizures after status epilepticus in mice lacking proapoptotic Puma. FASEB journal : official publication of the Federation of American Societies for Experimental Biology. 2010; 24:853–861. [PubMed: 19890018]

Freret T, Bouet V, Leconte C, Roussel S, Chazalviel L, Divoux D, Schumann-Bard P, Boulouard M. Behavioral deficits after distal focal cerebral ischemia in mice: Usefulness of adhesive removal test. Behavioral neuroscience. 2009; 123:224–230. [PubMed: 19170448]

Fujimoto M, Takagi Y, Aoki T, Hayase M, Marumo T, Gomi M, Nishimura M, Kataoka H, Hashimoto N, Nozaki K. Tissue inhibitor of metalloproteinases protect blood-brain barrier disruption in focal cerebral ischemia. Journal of cerebral blood flow and metabolism : official journal of the International Society of Cerebral Blood Flow and Metabolism. 2008; 28:1674–1685.

Gomez-Sanchez JC, Delgado-Esteban M, Rodriguez-Hernandez I, Sobrino T, Perez de la Ossa N, Reverte S, Bolanos JP, Gonzalez-Sarmiento R, Castillo J, Almeida A. The human Tp53 Arg72Pro polymorphism explains different functional prognosis in stroke. The Journal of experimental medicine. 2011; 208:429–437. [PubMed: 21357744]

Green DR. At the gates of death. Cancer cell. 2006; 9:328–330. [PubMed: 16697952]

Greig NH, Mattson MP, Perry T, Chan SL, Giordano T, Sambamurti K, Rogers JT, Ovadia H, Lahiri DK. New therapeutic strategies and drug candidates for neurodegenerative diseases: p53 and TNF-alpha inhibitors, and GLP-1 receptor agonists. Annals of the New York Academy of Sciences. 2004; 1035:290–315. [PubMed: 15681814]

Gudkov AV, Komarova EA. Prospective therapeutic applications of p53 inhibitors. Biochemical and biophysical research communications. 2005; 331:726–736. [PubMed: 15865929]

Gudkov AV, Komarova EA. Pathologies associated with the p53 response. Cold Spring Harbor perspectives in biology. 2010; 2:a001180. [PubMed: 20595398]

Hu X, Li P, Guo Y, Wang H, Leak RK, Chen S, Gao Y, Chen J. Microglia/macrophage polarization dynamics reveal novel mechanism of injury expansion after focal cerebral ischemia. Stroke; a journal of cerebral circulation. 2012; 43:3063–3070.

Hughes PE, Alexi T, Schreiber SS. A role for the tumour suppressor gene p53 in regulating neuronal apoptosis. Neuroreport. 1997; 8:v–xii. [PubMed: 9351639]

Jonkers J, Meuwissen R, van der Gulden H, Peterse H, van der Valk M, Berns A. Synergistic tumor suppressor activity of BRCA2 and p53 in a conditional mouse model for breast cancer. Nature genetics. 2001; 29:418–425. [PubMed: 11694875]

Kim WR, Sun W. Programmed cell death during postnatal development of the rodent nervous system. Development, growth & differentiation. 2011; 53:225–235.

Leker RR, Aharonowiz M, Greig NH, Ovadia H. The role of p53-induced apoptosis in cerebral ischemia: effects of the p53 inhibitor pifithrin alpha. Experimental neurology. 2004; 187:478–486. [PubMed: 15144874]

Li S, Overman JJ, Katsman D, Kozlov SV, Donnelly CJ, Twiss JL, Giger RJ, Coppola G, Geschwind DH, Carmichael ST. An age-related sprouting transcriptome provides molecular control of axonal sprouting after stroke. Nature neuroscience. 2010; 13:1496–1504. [PubMed: 21057507]

Li Y, Chopp M, Powers C, Jiang N. Apoptosis and protein expression after focal cerebral ischemia in rat. Brain research. 1997; 765:301–312. [PubMed: 9313903]

Li Y, Chopp M, Zhang ZG, Zaloga C, Niewenhuis L, Gautam S. p53-immunoreactive protein and p53 mRNA expression after transient middle cerebral artery occlusion in rats. Stroke; a journal of cerebral circulation. 1994; 25:849–855. discussion 855-846.

Liu F, Schafer DP, McCullough LD. TTC, fluoro-Jade B and NeuN staining confirm evolving phases of infarction induced by middle cerebral artery occlusion. Journal of neuroscience methods. 2009; 179:1–8. [PubMed: 19167427]

Love S. Apoptosis and brain ischaemia. Progress in neuro-psychopharmacology & biological psychiatry. 2003; 27:267–282. [PubMed: 12657366]

Luo Y, Kuo CC, Shen H, Chou J, Greig NH, Hoffer BJ, Wang Y. Delayed treatment with a p53 inhibitor enhances recovery in stroke brain. Annals of neurology. 2009; 65:520–530. [PubMed: 19475672]

Luo Y, Shen H, Liu HS, Yu SJ, Reiner DJ, Harvey BK, Hoffer BJ, Yang Y, Wang Y. CART peptide induces neuroregeneration in stroke rats. Journal of cerebral blood flow and metabolism : official journal of the International Society of Cerebral Blood Flow and Metabolism. 2013; 33:300–310.

Marchenko ND, Zaika A, Moll UM. Death signal-induced localization of p53 protein to mitochondria. A potential role in apoptotic signaling. The Journal of biological chemistry. 2000; 275:16202–16212. [PubMed: 10821866]

Minichiello L, Korte M, Wolfer D, Kuhn R, Unsicker K, Cestari V, Rossi-Arnaud C, Lipp HP, Bonhoeffer T, Klein R. Essential role for TrkB receptors in hippocampus-mediated learning. Neuron. 1999; 24:401–414. [PubMed: 10571233]

Neitemeier S, Ganjam GK, Diemert S, Culmsee C. Pifithrin-provides neuroprotective effects at the level of mitochondria independently of p53 inhibition. Apoptosis. 2014; 19

Nijboer CH, Heijnen CJ, van der Kooij MA, Zijlstra J, van Velthoven CT, Culmsee C, van Bel F, Hagberg H, Kavelaars A. Targeting the p53 pathway to protect the neonatal ischemic brain. Annals of neurology. 2011; 70:255–264. [PubMed: 21674585]

Perry VH, Nicoll JA, Holmes C. Microglia in neurodegenerative disease. Nature reviews Neurology. 2010; 6:193–201. [PubMed: 20234358]

Plesnila N, von Baumgarten L, Retiounskaia M, Engel D, Ardeshiri A, Zimmermann R, Hoffmann F, Landshamer S, Wagner E, Culmsee C. Delayed neuronal death after brain trauma involves p53-dependent inhibition of NF-kappaB transcriptional activity. Cell death and differentiation. 2007; 14:1529–1541. [PubMed: 17464322]

Popp A, Jaenisch N, Witte OW, Frahm C. Identification of ischemic regions in a rat model of stroke. PloS one. 2009; 4:e4764. [PubMed: 19274095]

Rachmany L, Tweedie D, Rubovitch V, Yu QS, Li Y, Wang JY, Pick CG, Greig NH. Cognitive impairments accompanying rodent mild traumatic brain injury involve p53-dependent neuronal cell death and are ameliorated by the tetrahydrobenzothiazole PFT-alpha. PloS one. 2013; 8:e79837. [PubMed: 24312187]

Rios M, Fan G, Fekete C, Kelly J, Bates B, Kuehn R, Lechan RM, Jaenisch R. Conditional deletion of brain-derived neurotrophic factor in the postnatal brain leads to obesity and hyperactivity. Molecular endocrinology. 2001; 15:1748–1757. [PubMed: 11579207]

Saelens X, Festjens N, Vande Walle L, van Gurp M, van Loo G, Vandenabeele P. Toxic proteins released from mitochondria in cell death. Oncogene. 2004; 23:2861–2874. [PubMed: 15077149]

Sano T, Reynolds JP, Jimenez-Mateos EM, Matsushima S, Taki W, Henshall DC. MicroRNA-34a upregulation during seizure-induced neuronal death. Cell death & disease. 2012; 3:e287. [PubMed: 22436728]

Shen H, Luo Y, Kuo CC, Wang Y. BMP7 reduces synergistic injury induced by methamphetamine and ischemia in mouse brain. Neuroscience letters. 2008; 442:15–18. [PubMed: 18598737]

Shen H, Wang Y. Correlation of locomotor activity and brain infarction in rats with transient focal ischemia. Journal of neuroscience methods. 2010; 186:150–154. [PubMed: 19917312]

Shinozuka K, Dailey T, Tajiri N, Ishikawa H, Kim DW, Pabon M, Acosta S, Kaneko Y, Borlongan CV. Stem Cells for Neurovascular Repair in Stroke. Journal of stem cell research & therapy. 2013; 4:12912. [PubMed: 24077523]

Smith JA, Park S, Krause JS, Banik NL. Oxidative stress, DNA damage, and the telomeric complex as therapeutic targets in acute neurodegeneration. Neurochemistry international. 2013; 62:764–775. [PubMed: 23422879]

Strom E, Sathe S, Komarov PG, Chernova OB, Pavlovska I, Shyshynova I, Bosykh DA, Burdelya LG, Macklis RM, Skaliter R, Komarova EA, Gudkov AV. Small-molecule inhibitor of p53 binding to mitochondria protects mice from gamma radiation. Nature chemical biology. 2006; 2:474–479. [PubMed: 16862141]

Swanson RA, Morton MT, Tsao-Wu G, Savalos RA, Davidson C, Sharp FR. A semiautomated method for measuring brain infarct volume. Journal of cerebral blood flow and metabolism : official journal of the International Society of Cerebral Blood Flow and Metabolism. 1990; 10:290–293.

Tedeschi A, Di Giovanni S. The non-apoptotic role of p53 in neuronal biology: enlightening the dark side of the moon. EMBO reports. 2009; 10:576–583. [PubMed: 19424293]

Zheng Z, Zhao H, Steinberg GK, Yenari MA. Cellular and molecular events underlying ischemia-induced neuronal apoptosis. Drug news & perspectives. 2003; 16:497–503. [PubMed: 14668947]

Zhu X, Yu QS, Cutler RG, Culmsee CW, Holloway HW, Lahiri DK, Mattson MP, Greig NH. Novel p53 inactivators with neuroprotective action: syntheses and pharmacological evaluation of 2-imino-2,3,4,5,6,7-hexahydrobenzothiazole and 2-imino-2,3,4,5,6,7-hexahydrobenzoxazole derivatives. Journal of medicinal chemistry. 2002; 45:5090–5097. [PubMed: 12408720]

Highlights

- A forebrain neuronal specific p53 ko mouse model to evaluate direct involvement of p53 in neurons.

- p53 expression upregulation in the ischemic neuronal cells in wt mice but not CamcreTRP53 ko mice.

- Deletion of the p53 gene in forebrain neurons results in decreased infarction area in ko mice.

- Deletion of the p53 gene in forebrain neurons results in less severe locomotor deficits in ko mice.

- Neuronal-specific inhibition of p53 might provide a new treatment strategy for improved prognosis.

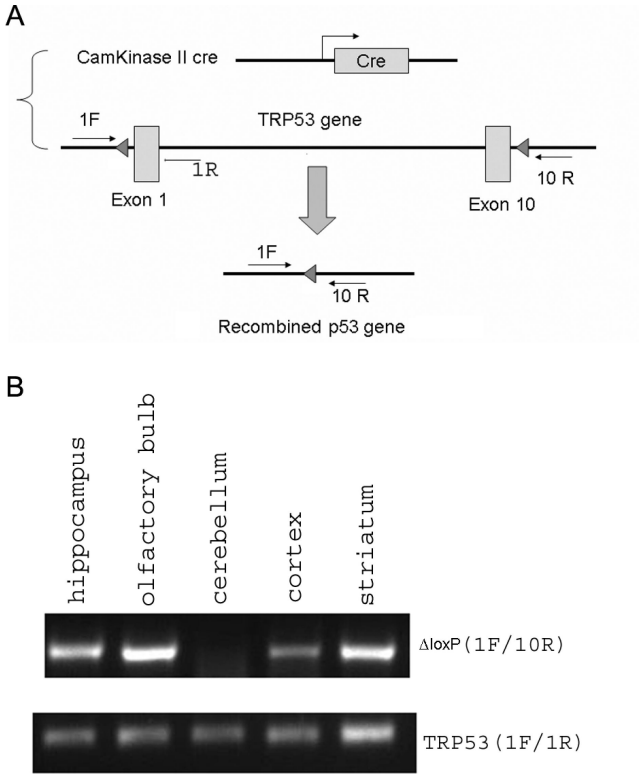

Figure 1.

A. Strategy for forebrain neuronal specific deletion of the p53 gene in CamcreTRP53 ko mice. B. Detection of recombined alleles (indicating deletion of p53 gene) in hippocampus, olfactory bulb, cortex and striatum but not in cerebellum of ko mice (upper panel), detection of loxP flanked alleles in all genomic DNA samples that confirm the genotype and quality of extracted genomic DNA.

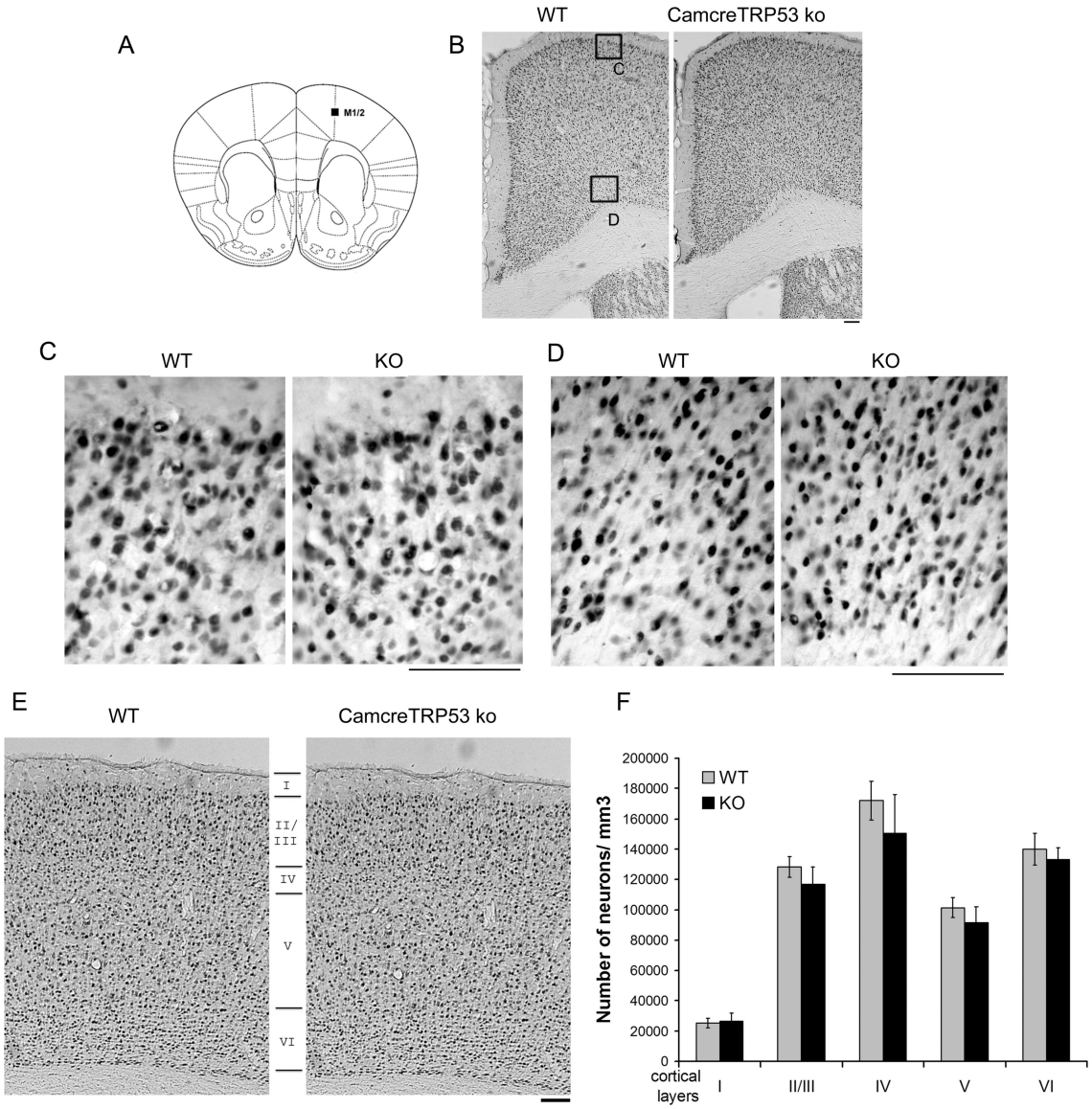

Figure 2.

A) Brain schematic showing the motor cortex area examined in images. B) no apparent abnormality in general structure by NeuN positive neuron distribution in motor cortex in ko mice. C, D showing higher magnifications of the areas indicated in panel B. E showing layer I through VI in neocortex of wt and ko mice. F showing neuronal cell density in each layers of cortex measured using stereological methods. Scale bar =100 um.

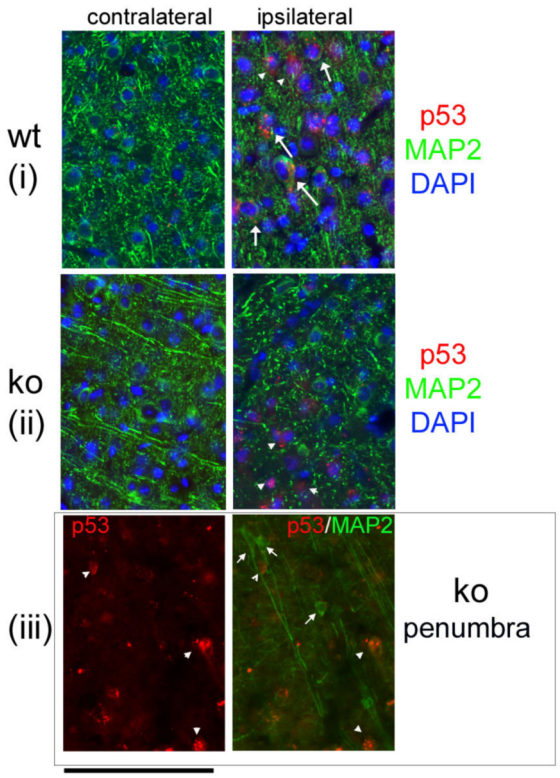

Figure 3.

p53 protein is detected in ischemic penumbra in wt mice both in MAP2 positive and MAP2 negative cells (arrow and arrow head, Panel i right) but is not detected in the contralateral cortex (panel i and ii left). In CamcreTRP53 ko mice, p53 protein is mainly detected in MAP2 negative cells but not in neurons (panel ii right, arrow heads). We also identified some surviving MAP2 positive neurons near the ischemic core that are negative for p53 expression (panel iii left and right, short arrow). Scale bar =100 um

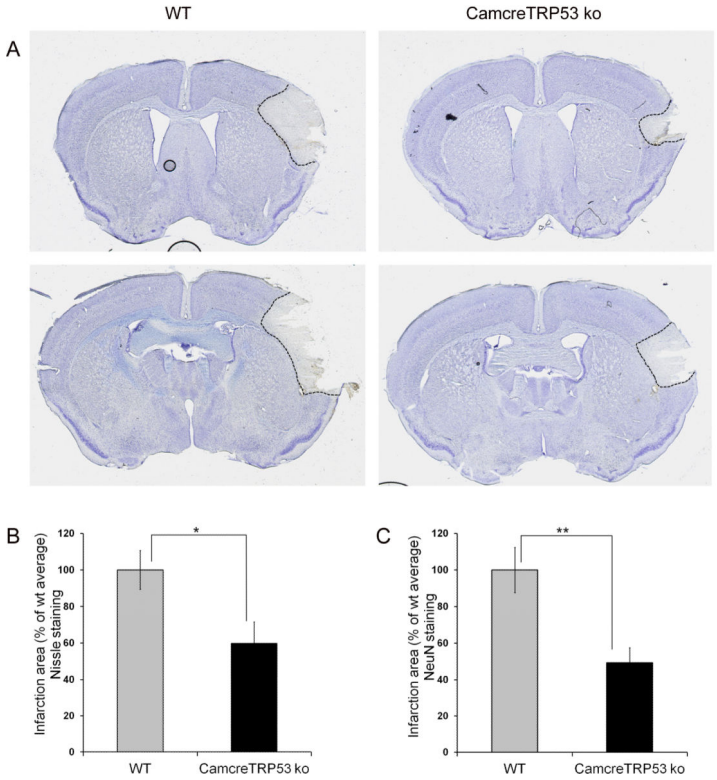

Figure 4.

Forebrain neuronal specific p53 deletion results in decreased infarction size in CamcreTRP53 ko mice as quantified by Nissl staining (panel A and B) and loss of NeuN positive neurons in the ipsilateral cortex (panel C). (* indicating $p<0.05$ and ** indicating $p<0.01$, n=15).

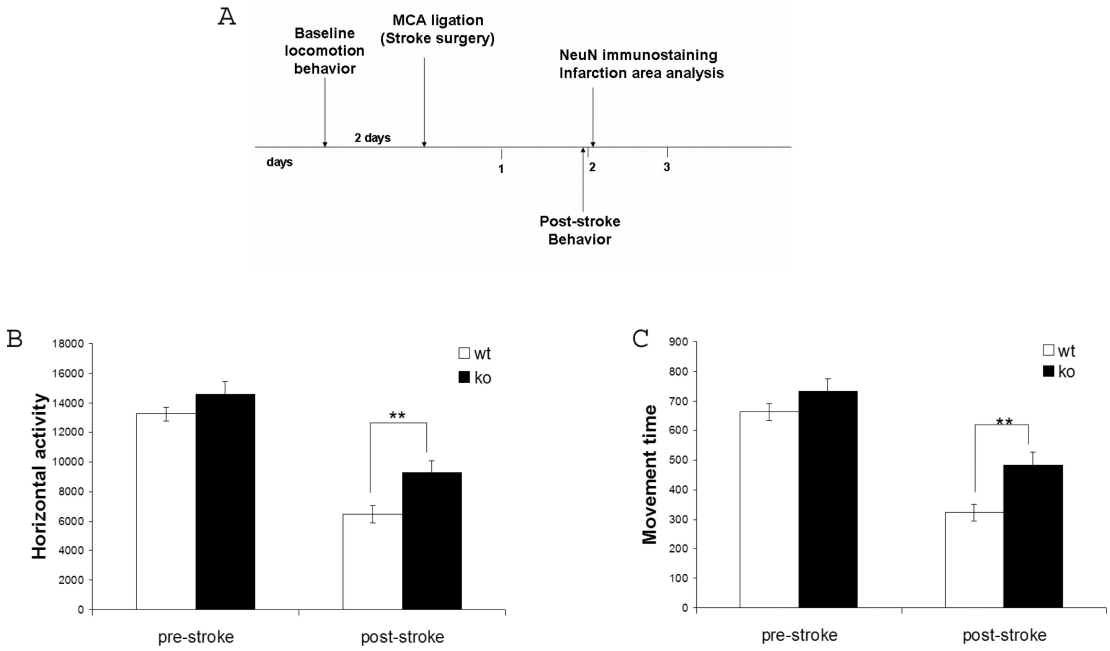

Figure 5.

A. Timeline for behavioral and histological measurements. CamcreTRP53 ko mice showed no difference from wt littermates in locomotion measured before MCAo. At 48 hr post MCAo, CamcreTRP53 ko mice demonstrated less deficits in motor function compared to wt mice, indicated both by total horizontal activity during 30 min (panel B) and total movement time during 30 min (panel C). ** indicates $p < 0.01$, n= 17 for wt and 16 for ko.

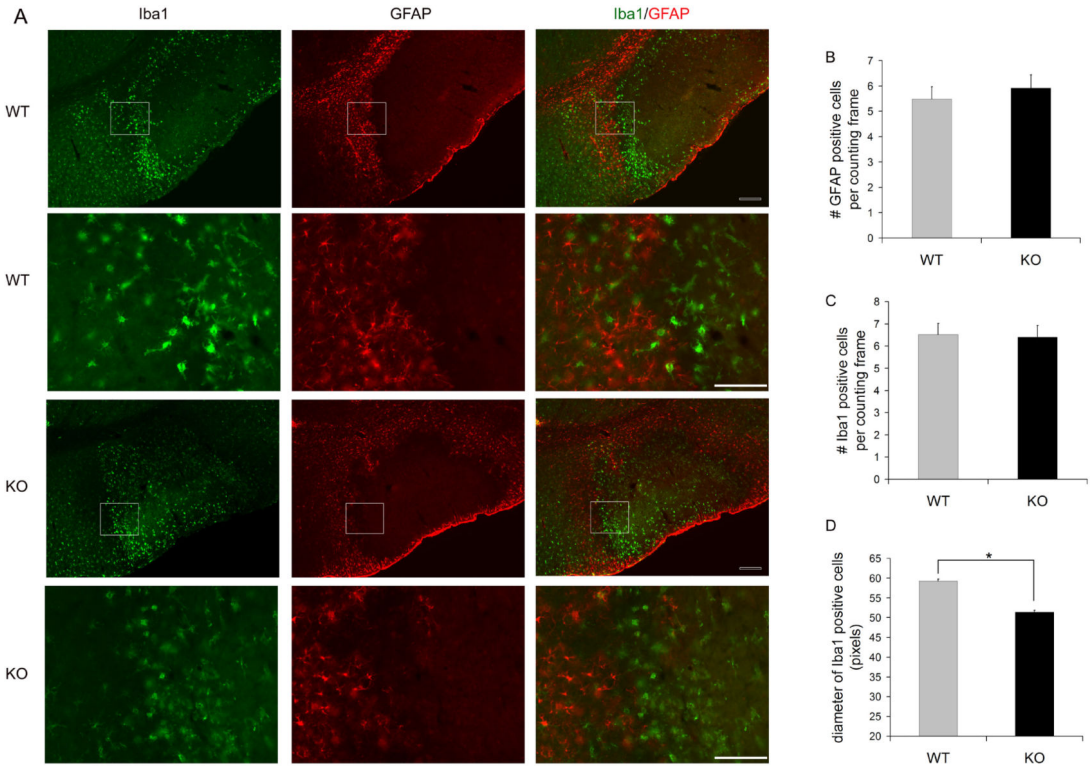

Figure 6.

Reactive astrocytes (GFAP positive) and activated microglia (Iba1 positive) were observed in the periinfarct area in ischemic brains of wt and CamcreTRP53 mice (panel A). The number of activated astrocytes (panel B) and microglia (panel C) are similar in wt and ko mice but microglial cells in ko mice have a smaller cell body size measured by diameter of Iba1 positive cells (panel D). * indicates $p<0.05$, n=5 animals per group with >150 total cells measured. Scale bar =200 um for smaller magnification images (row 1 and 3) and 100um for larger magnification images (row 2 and 4).

Table 1

Locomotor behavior parameters in wildtype and CamcreTRP53 ko mice before and 48 hours after MCAo.

	Pre-stroke					Post-stroke				
	WT		CamcreTRP53 ko			WT		CamcreTRP53 ko		
	mean	s.e.m.	mean	s.e.m.	*p value	mean	s.e.m.	mean	s.e.m.	*p value
HACTV	13412.6	448.2	14573.6	845.6	>0.05	6752.6	568.9	9335.9	805.5	<0.05
TOTDIST	6652.7	403.0	8033.4	596.7	>0.05	2897.4	360.7	4760.1	529.3	<0.01
MOVNO	452.6	5.2	414.0	11.3	>0.05	307.1	18.2	358.9	24.4	<0.05
MOVTIME	674.1	27.6	732.3	43.8	>0.05	326.6	28.7	491.2	42.1	<0.01
RESTIME	1125.7	27.6	1067.6	43.8	>0.05	1473.2	28.7	1308.7	42.1	<0.01
VACTV	967.4	79.7	839.4	84.4	>0.05	388.4	66.1	555.5	86.4	>0.05
VMOVNO	274.3	16.1	255.8	17.4	>0.05	105.8	18.9	166.6	26.8	<0.05
STRCNT	9165.3	370.5	9867.6	689.8	>0.05	3915.3	398.5	5812.9	575.9	<0.05

HACTV (horizontal activity) = total number of beam interruptions that occurred in the horizontal sensors

TOTDIST (total distance travelled) = the total distance (cm) travelled.

MOVNO (number of movements) = the number of separate horizontal movements executed.

MOVTIME (movement time) = the amount of time (second) in ambulation.

RESTIME (rest time) = the amount of time (second) in rest.

VACTV (vertical activity) = total number of beam interruptions that occurred in the vertical sensors.

VMOVNO (vertical number of movements) = the number of separate vertical movements executed.

STRCNT (stereotypy counts) = the number of beam breaks that occur during this period of stereotypic activity.

*Difference between wt and ko mice within pre-stroke or post-stroke condition (All Pairwise Multiple Comparison Procedures using Student-Newman-Keuls Method).